

The Evolution of Kicked Stellar-Mass Black Holes in Star Cluster Environments

Jeremy J. Webb¹, Nathan W. C. Leigh², Abhishek Singh¹, K. E. Saavik Ford^{2,3,4,5}, Barry McKernan^{2,3,4,5}, Jillian Bellovary² *

¹*Department of Astronomy, Indiana University, Swain West, 727 E. 3rd Street, IN 47405 Bloomington, USA*

²*Department of Astrophysics, American Museum of Natural History, Central Park West and 79th Street, New York, NY 10024*

³*Department of Science, BMCC, City University of New York, New York, NY 10007, USA*

⁴*Graduate Center, City University of New York, 365 5th Avenue, New York, NY 10016, USA*

⁵*Kavli Institute for Theoretical Physics, UC Santa Barbara, CA 93106, US*

28 November 2017

ABSTRACT

We consider how dynamical friction acts on black holes that receive a velocity kick while located at the center of a gravitational potential, analogous to a star cluster, due to either a natal kick or the anisotropic emission of gravitational waves during a black hole-black hole merger. Our investigation specifically focuses on how well various Chandrasekhar-based dynamical friction models can predict the orbital decay of kicked black holes with $m_{bh} \lesssim 100M_{\odot}$ due to an inhomogeneous background stellar field. In general, the orbital evolution of a kicked black hole follows that of a damped oscillator where two-body encounters and dynamical friction serve as sources of damping. However, we find models for approximating the effects of dynamical friction do not accurately predict the amount of energy lost by the black hole if the initial kick velocity v_k is greater than the stellar velocity dispersion σ . For all kick velocities, we also find that two-body encounters with nearby stars can cause the energy evolution of a kicked BH to stray significantly from standard dynamical friction theory as encounters can sometimes lead to an energy gain. For larger kick velocities, we find the orbital decay of a black hole departs from classical theory completely as the black hole’s orbital amplitude decays linearly with time as opposed to exponentially. Therefore, we have developed a linear decay formalism which scales linearly with black hole mass and $\frac{v_k}{\sigma}$ in order to account for the variations in the local gravitational potential.

Key words: galaxies: nuclei – stars: black holes – black hole physics – methods: analytical – globular clusters: general.

1 INTRODUCTION

Black holes (BHs) are believed to receive velocity kicks both upon formation and as part of a BH-BH merger. When BHs form they receive a natal kick between 0 and 100 km/s, similar to the kicks received by neutron stars (Repetto et al. 2012). When two black holes (BHs) merge, they experience a kick due to the anisotropic emission of gravitational waves (GWs) (e.g. Favata, Hughes & Holz 2004; Merritt 2004; Blecha et al. 2011). The magnitude of the kick can vary by orders of magnitude depending on the binary mass ratio, BH spins and the relative angles of inclination between

the BH spin axes and the binary orbital plane. The kick velocities range from $\lesssim 1$ km/s to over 500 km/s, reaching a maximum at a mass ratio of $q \sim 0.3$ (Favata, Hughes & Holz 2004) for maximally misaligned spins. For very low mass ratios $q \lesssim 0.05$, the kick velocities are always small $\lesssim 100$ km/s, independent of the BH spins or their orientations relative to the binary orbital plane (see Figure 1 in Merritt (2004)).

The four gravitational wave detections to date have been attributed to the merger of BHs between 8 and 36 M_{\odot} (Abbott et al. 2016,b, 2017,b) which yield remnants with $m_{bh} \lesssim 100M_{\odot}$. The dense environments of globular clusters (GCs) represent the most likely host for such events through the merger of dynamically formed BH binaries. Mergers can occur throughout a GC’s lifetimes, from their infancy (e.g. Leigh et al. 2013a,b) to the

* E-mail: jerjwebb@iu.edu (JW); nleigh@amnh.org (NL); sford@amnh.org (KESF); bmckernan@amnh.org (BM); jbellovary@amnh.org (JB)

present-day age of the host galaxy (e.g. Rodriguez et al. 2015, 2016; Leigh, Geller & Toonen 2016). Nuclear star clusters (NSCs) (e.g. Miller & Lauburg 2008; Antonini & Rasio 2016) and the massive gas disks in active galactic nuclei (AGN) (McKernan et al. 2017) have also been suggested as likely locations for stellar BH mergers. Within these dense environments, BHs should undergo frequent mergers with other BHs (Sippel & Hurley 2013). Although the exact details of how intermediate massive BHs (IMBHs) (e.g. Bahcall & Ostriker 1975; Portegies Zwart et al. 2004; Gratton, Carretta & Bragaglia 2012; Leigh et al. 2013a,b, 2014) and supermassive BH (SMBHs) (e.g. Oh & Haiman 2002; Bromm & Loeb 2003; Volonteri & Rees 2005; Shapiro 2005; Wise & Abel 2008; Shang, Bryan & Haiman 2010; Tanaka & Li 2014; Madau & Rees 2001; Haiman & Loeb 2001; Volonteri & Rees 2006; Tanaka & Haiman 2009) form and grow are poorly understood.

An abundance of observational evidence now exists in favour of the actual existence of BHs in these dense stellar environments. However, the observational evidence in favour of stellar-mass BHs and SMBHs is more compelling than for IMBHs. For example, in the giant elliptical galaxy NGC 4472 in the Virgo Cluster, Maccarone et al. (2007) reported an accreting BH in an associated GC. The X-ray luminosity is so high that the authors argue it cannot be anything other than a BH. Shortly thereafter, Shih et al. (2010) reported an accreting BH in a GC hosted by the giant elliptical galaxy NGC 1399 at the centre of the Fornax Cluster. As for stellar-mass BHs in GCs, Strader et al. (2012) recently reported the detection of two flat-spectrum radio sources in the Galactic GC M22. If confirmed, these two detections could imply the presence of more unseen BHs, somewhere in the range $\sim 5 - 100$ in M22. Even more recently, Chomiuk et al. (2013) reported a candidate BH X-ray binary in the Galactic GC M62. Finally, Peuten et al. (2016) used N -body star cluster simulations to demonstrate that the lack of mass segregation in NGC 6101 could be the result of the cluster having a larger stellar-mass BH population.

Understanding the orbital behaviour of newly formed BHs and BH merger remnants that receive velocity kicks due to gravitational wave recoil at the centre of their host potential (which can either be a star cluster or a galaxy) is essential to understanding how gravitational waves are produced and how massive BHs may form and evolve. In this paper, we specifically explore the behaviour of kicked BHs in star cluster environments with masses that are comparable to the sources of all four gravitational wave detections. We also investigate how well classic dynamical friction theory (Chandrasekhar 1943) predicts the orbital decay of a kicked BH. Several studies have already attempted to model the evolution of a BH that has been given a velocity kick and is subject to dynamical friction, however they have been forced to restrict the parameter space to either near-zero velocity kicks (Chatterjee et al. 2002) or high BH masses (Gualandris & Merritt 2008) in order to develop an analytic model for how the BH's energy (and therefore its position and velocity) evolves with time. An analytic model to describe as a function of time the displacement from $r = 0$ of a kicked massive BH, no matter the initial kick velocity or BH mass, will have direct implications for observations of BHs/IMBHs in GCs and NSCs, SMBHs in galactic nuclei, and gravitational wave detections. Modelling the orbital de-

cay of kicked BHs will also help constrain theoretical models attempting to describe the formation, merger rate and subsequent growth of BHs.

In Section 2, we derive the equations of motion for a BH located at $r = 0$ that is imparted with a kick at $t = 0$, assuming a Plummer sphere for the gravitational potential. Section 3 is then dedicated to introducing the N -body simulations we use to determine how well derived equations of motion predict the behaviour of kicked BHs in star clusters. We then compare our model, as well as the models of Chatterjee et al. (2002) and Gualandris & Merritt (2008) to our N -body simulations in Section 4. In Section 5 we address discrepancies between the theory and simulations and introduce a new formalism to properly model the evolution of BHs with $m_{bh} \lesssim 100M_{\odot}$. The formalism is applicable over the entire range of BH masses and kick velocities explored in this study. Finally, we summarize our main conclusions and discuss the implications of our results in Section 6.

2 THEORY

The initial mass function of star clusters is such that hundreds of BHs will form early in the cluster's lifetime (Salpeter 1955; Kroupa, Tout, & Gilmore 1993; Kroupa 2001). Natal velocity kicks between 0 and 100 km/s are such that approximately 10% of all BHs are retained by the cluster (Pfahl et al. 2002; Pfahl 2003). Over time, kicked BHs will sink to the core of the cluster through dynamical friction and two-body interactions. While some BHs will be subsequently kicked from the cluster due to BH-BH interactions, Sippel & Hurley (2013) found that just over 30% of all retained BHs will remain in the cluster after a Hubble time as either single BHs, part of a binary system with a main sequence star, or part of a BH-BH binary.

Of the BHs that form BH-BH binaries, only a fraction will merge while still within the cluster while others will be kicked from the cluster due to three-body scattering before merging (Askar et al. 2017; Banerjee 2017a,b). Askar et al. (2017) suggests that the fraction of BH-BH mergers occurring within the cluster may be as low as 15%. As previously mentioned, when a BH-BH binary merges the velocity kick imparted on the merger product can be anywhere from 1 km/s to over 500 km/s. Hence, when mergers occur only a small fraction of BH-BH merger products will be retained by the cluster and will later form a new, more massive, BH-BH binary that will also eventually merge. Similar to newly formed BHs, dynamical friction and two-body interactions will force retained merger products to sink to the core again so the process can repeat. However, it should be noted that only a small fraction of all BHs produced in a cluster will reach the necessary masses to produce the gravitational wave detections produced by LIGO.

To better constrain the ability and timescale over which repeated BH-BH mergers will occur within star clusters, it is important to understand how effectively dynamical friction can return kicked BHs to the core. Chandrasekhar (1943) was the first to derive the loss of energy via dynamical friction that a test body of mass M will experience due to a *homogeneous* background distribution of stars of mass m_s . Given that the test body has a velocity v_M , the force of dynamical friction on the test body can be written as:

$$F_{DF} = -\beta v_M \quad (1)$$

where β equals (Binney & Tremaine 1987):

$$\beta = 16\pi^2 \ln\Lambda G^2 M m_s \frac{\int_0^{v_M} f(r, u) u^2 du}{v_M^3} \quad (2)$$

In Equation 2, $\ln\Lambda$ is the Coulomb logarithm and $f(r, u)$ is the phase space distribution function of stellar positions r and velocities u . However it should be noted that the calculations are just as easily applicable to a test body losing energy via dynamical friction due to a background gaseous field.

Several studies have considered the scenario of the test body travelling through a non-homogeneous stellar field, including cases where the test body passes through or is located at the minimum of a gravitational potential. Such a scenario directly applies to star clusters and satellite galaxies orbiting around a central host (e.g. Ostriker, Binney & Saha 1989; Pesce, Capuzzo-Dolcetta & Vietri 1989; Colpi et al. 1999; Fujii et al. 2006; Cole et al. 2012; Arca-Sedda & Capuzzo-Dolcetta 2014a,b; Brockamp et al. 2014) and BHs orbiting within the background stellar field of either a star cluster or galaxy (e.g. Chatterjee et al. 2002; Vicari, Capuzzo-Dolcetta & Merritt 2007; Gualandris & Merritt 2008; Antonini & Merritt 2012). In these cases, the mass of the test body is significantly higher than the mean mass of stars in the stellar field but only a fraction of the total mass of the stellar system.

Several of the above studies have found that the early work of Chandrasekhar (1943) can be inaccurate when applied to test bodies in non-homogeneous stellar fields (Ostriker, Binney & Saha 1989; Pesce, Capuzzo-Dolcetta & Vietri 1989; Colpi et al. 1999; Antonini & Merritt 2012; Arca-Sedda & Capuzzo-Dolcetta 2014a,b; Vicari, Capuzzo-Dolcetta & Merritt 2007). Hence new treatments for the dynamical friction of test bodies in dense stellar systems have been developed to estimate in-fall times (Antonini & Merritt 2012; Arca-Sedda & Capuzzo-Dolcetta 2014a). Recently, the works of Antonini & Merritt (2012) and Arca-Sedda & Capuzzo-Dolcetta (2014a) have been demonstrated to be applicable to the inner regions of galaxies (Antonini 2014; Arca-Sedda et al. 2015) and star clusters (Arca-Sedda 2016) respectively.

We continue exploring the scenario of test bodies in non-homogeneous stellar fields by applying the work of Chandrasekhar (1943) to newly formed BHs and BH-BH merger remnants orbiting within a star cluster environment. The resulting BH will have a mass $m_{BH} \gg m$, where m is the mean stellar mass in the surrounding star cluster. We assume the remnant is formed at time $t = 0$ with a velocity kick of magnitude v_{kick} that is less than the escape velocity v_{esc} from $r = 0$.

In order to obtain a solution for the displacement from $r = 0$ or the position of the kicked BH $r(t)$ as a function of time t , we begin by writing the equation of motion for the BH. This is done by balancing the forces acting on the BH, beginning immediately after the BH receives a kick at $t = 0$ and $r = 0$:

$$F_{tot} = F_g + F_{DF}, \quad (3)$$

where F_g is the gravitational force and F_{DF} is the damping force, which we take as being equal to the stellar dynamical friction force F_{sDF} (note that we have absorbed the force direction into the terms F_g and F_{sDF} ; see below). Several studies have attempted to simplify Equation 2 such that the exact form of the distribution function does not need to be known (e.g. Chatterjee et al. 2002; Gualandris & Merritt 2008). The first key assumption that needs to be made moving forward is the functional form of the background potential. For the purposes of this study, we will assume the background stellar field can be approximated as a Plummer Sphere, which has been used to describe open clusters, GCs and galactic bulges.

For a Plummer sphere, the gravitational potential and density are, respectively:

$$\Phi(r) = -\frac{GM}{\sqrt{r^2 + a^2}} = -\frac{GM}{a} \left(1 + \frac{r^2}{a^2}\right)^{-1/2} \quad (4)$$

and

$$\rho(r) = \frac{3M}{4\pi a^3} \left(1 + \frac{r^2}{a^2}\right)^{-5/2}, \quad (5)$$

where M is the total cluster mass, a is the Plummer radius or scale length and r is the distance from the cluster centre. For a Plummer sphere, the velocity dispersion takes on its maximum value at $r = a$, or:

$$\sigma(a) = \left(\frac{GM}{2\sqrt{2}a}\right)^{1/2} \quad (6)$$

The specific gravitational force F_g acting on the kicked BH is calculated from the gradient of the gravitational potential:

$$F_g = -\frac{d\Phi}{dr} = \frac{GMr}{a^3} \left(1 + \frac{r^2}{a^2}\right)^{-3/2} \quad (7)$$

Similarly, the specific stellar dynamical friction force acting on the BH is (Chandrasekhar 1943):

$$F_{sDF} = -\frac{4\pi G^2 m_{BH} \ln\Lambda \rho(r)}{v^2}, \quad (8)$$

where $v = \dot{r} = dr/dt$ is the (magnitude of the) velocity of the BH with respect to the cluster centre, and $\ln\Lambda$ is the Coulomb logarithm. Note that we take $\ln\Lambda$ from Chatterjee et al. (2002), who specifically derives the Coloump logarithm for a Plummer sphere. Plugging Equations 7 and 8 into Equation 3 gives:

$$\ddot{r} + \frac{3G^2 M m_{BH} \ln\Lambda}{a^3} \left(1 + \frac{r^2}{a^2}\right)^{-5/2} r^{-2} + \frac{GM}{a^3} \left(1 + \frac{r^2}{a^2}\right)^{-3/2} r = 0 \quad (9)$$

Note that we are implicitly assuming that only the BH moves in our model. The cluster potential and centre of mass are assumed to be static in time and space.

Equation 9 is a second-order ordinary differential equation which must be solved numerically. In order to obtain an analytic solution, simplifying assumptions must be made in addition to assuming that the stellar field can be approximated by a Plummer Sphere and that $m_{bh} \gg m_s$. For the purposes of this study, we will first consider the special cases of a BH following a 1D trajectory and:

- The BH is given a low initial velocity at the origin of the background potential such that it stays within the Plummer Sphere’s scale radius.

- The BH is undergoing Brownian motion near the origin of the background potential (Chatterjee et al. 2002).

- The BH is massive compared to nearby stars and is given a larger velocity kick such that its location within the background potential is not restricted (Gualandris & Merritt 2008).

In each section we describe the necessary assumptions and defer a more thorough discussion of their justification and astrophysical significance to Section 5.

2.1 Low Velocity Kicks at the Origin

By assuming that the motion of the kicked BH follows a 1D trajectory, we set $\dot{r} = 0$ at the turn-around points. This is not accounted for in Equation 8; the dynamical friction force blows up at zero velocity. To correct for this we take the simple, yet unphysical, approach of adding an additional term to the velocity in the denominator of Equation 8, namely the product of the stellar velocity dispersion σ . That is, we replace $\dot{r}v^{-3}$ with $\dot{r}(v^2 + \sigma^2)^{-3/2}$. This gives:

$$F_{\text{sDF}} = -\frac{4\pi G^2 m_{\text{BH}} \ln \Lambda \rho(r) \dot{r}}{(\sigma^3)} \left(1 + \frac{\dot{r}^2}{\sigma^2}\right)^{-3/2}. \quad (10)$$

As required, Equation 10 gives $F_{\text{sDF}} = 0$ when $v = 0$, and is otherwise negative. For examples of more rigorous and dynamically motivated treatments for Equation 8 diverging as \dot{r} goes to 0, see Just et al. (2011), Antonini & Merritt (2012), and Arca-Sedda & Capuzzo-Dolcetta (2014a).

Next we assume that the BH is restricted to the limiting case $v_{\text{kick}} \ll \sigma$ in order to get the last term in Equation 10 to asymptote to unity. Under this assumption, we obtain:

$$F_{\text{sDF}} = -\frac{4\pi G^2 m_{\text{BH}} \ln \Lambda \rho(r) \dot{r}}{\sigma^3} \quad (11)$$

Similarly, if we assume that the motion of the kicked BH is restricted to $r \ll a$, then Equation 7 simplifies to:

$$F_{\text{g}} = -\frac{d\Phi}{dr} = \frac{GM}{a^3} r \quad (12)$$

Plugging Equations 11 and 12 back into Equation 9 now yields an equation of the general form:

$$\ddot{r} - b\dot{r} - kr = 0, \quad (13)$$

Equation 13 has a well known solution, namely that of the damped simple harmonic oscillator. That is, in the limits $\dot{r} \leq v_{\text{kick}} = \dot{r}(t=0) \ll \sigma$ and $r \ll a$, the solution to Equation 9 is:

$$r(t) = Ae^{-bt/2} \sin(\omega_{\text{DF}} t), \quad (14)$$

where the constants are

$$b = \frac{3G^2 m_{\text{BH}} M \ln \Lambda}{\sigma^3 a^3} \quad (15)$$

and

$$k = \frac{GM}{a^3} \quad (16)$$

The damping frequency is:

$$\omega_{\text{DF}} = \omega_0 \left(1 - \frac{b^2}{4k}\right)^{1/2}, \quad (17)$$

where $\omega_0 = \sqrt{k}$ is the natural (undamped) frequency. Equation 14 is subject to the boundary conditions $r(0) = 0$ and $\dot{r}(0) = v_{\text{kick}} = \dot{r}_0$, which gives for the amplitude of oscillation:

$$A = \frac{\dot{r}_0}{\omega_{\text{DF}}} \quad (18)$$

Equation 14 together with Equations 15, 16, 17 and 18 give the position of the BH at any time t after receiving a kick at the origin, in the limit $\dot{r}_0 = v_{\text{kick}} \ll \sigma$ and $r \ll a$ (i.e. for small BH kicks). This should frequently be the case for mergers between stellar-mass BHs and either IMBHs or SMBHs at the centres of, respectively, massive GCs and galactic nuclei.

2.1.1 Over-Damped versus Under-Damped Oscillation

Equation 17 can also be used to qualify the BH’s behaviour by comparing it to the *BH’s relaxation time* (Equation 19), which corresponds roughly to the time required for the BH to reach its final kinetic energy, or (approximate) orbit within the cluster, at which point the rate of dynamical heating of the BH due to random perturbations with other stars is balanced by the rate of cooling due to dynamical friction.¹ It can be calculated using Equation 3.2 in Merritt (2013) at $r = a$:

$$\tau_{\text{rh}}(m_{\text{BH}}) = \frac{m}{m_{\text{BH}}} \tau_{\text{rh}}(m), \quad (19)$$

where

$$\tau_{\text{rh}}(m) = 0.34 \frac{\sigma(a)^3}{G^2 m \rho(a) \ln \Lambda}, \quad (20)$$

where $\rho(a)$ and $\sigma(a)$ are the Plummer density and velocity dispersion, respectively, evaluated at $r = a$. Equations 5 and 6 can be plugged into Equation 20, and subsequently into Equation 19, which can then be re-written as:

$$\tau_{\text{rh}}(m_{\text{BH}}) = \frac{0.91 \pi M^{1/2} a^2}{G^{1/2} m_{\text{BH}} \ln \Lambda}. \quad (21)$$

We will henceforth refer to Equation 21 as the *BH relaxation time*. Equation 21 roughly describes the time required for the kicked BH to become fully damped, to within a factor of ~ 2 .

In Figure 1, we show by the solid line the critical BH mass m_{BH} at which the oscillator is critically damped, as a function of the total cluster mass M . That is, the solid

¹ When this equilibrium is reached, the final steady-state BH velocity should be $v \sim (m/m_{\text{BH}})^{1/2} \sigma$, however recent studies have found the $\frac{1}{2}$ power is too high by a factor of ~ 2 (Trenti & van der Marel 2013).

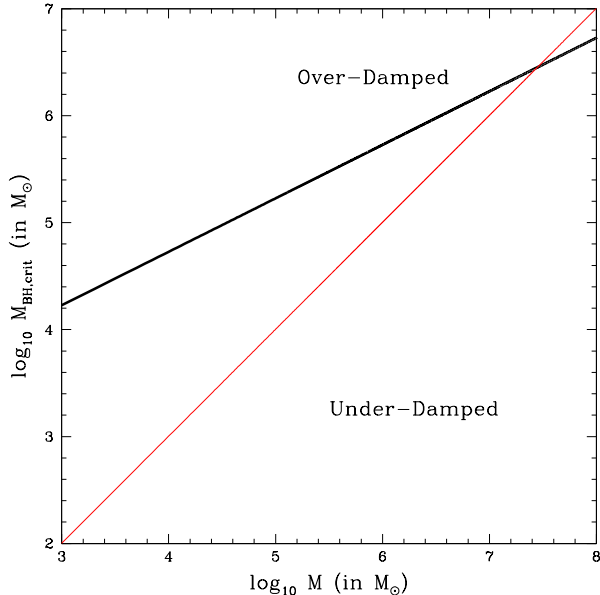


Figure 1. The black line shows the (logarithm of the) BH mass corresponding to a critically damped oscillator, for which the BH is fully relaxed after only a single oscillation, as a function of the (logarithm of the) total cluster mass. For comparison, the red line shows the BH mass for which the crossing time within the Plummer radius is equal to the BH relaxation time. All masses are shown in solar masses.

black line corresponds to the "critical" BH mass at which the BH's relaxation time is equal to the period of oscillation, $2\pi/\omega_{DF}$. Above this line the cluster's relaxation time is shorter than the BH's orbital period, such that the cluster's internal dynamics will return the BH to the origin very quickly and it will behave as an over-damped oscillator. For a BH which falls below the line, it will be able to undergo several complete orbits and have its orbit decay due to dynamical friction before the cluster's internal dynamics begin to play an important role. Hence it will behave as an under-damped oscillator. For comparison we also show by the red line the critical BH mass at which the crossing time, which can also be used as a tracer of a cluster's dynamical age, inside the Plummer radius is equal to the BH relaxation time. Importantly, Figure 1 is valid only for small kick velocities satisfying $v_{kick} < \sigma$.

2.2 Brownian Motion

Chatterjee et al. (2002) applied the work of Chandrasekhar (1943) to the dynamics of a MBH undergoing Brownian motion near the center of a dense stellar system characterized by a Plummer sphere of mass M and scale radius a . Since the distribution function varies slowly with r near the center of a Plummer sphere, the authors also used Equation 2 under the assumption that $r_{bh} \ll a$ at all times. Hence the background potential can be approximated to be $\Phi = -\frac{GM_P}{a}$. Furthermore, since the authors were not focused on the BH undergoing oscillatory motion, they did not have to adjust their derivation to take into account F_{DF} going to infinity at zero velocity as was done in Equation 15.

Assuming the MBH moves very slowly compared to nearby stars, Chatterjee et al. (2002) instead reduces Equation 2 to:

$$\beta = \frac{128\sqrt{2}}{7\pi} \ln\Lambda \left(\frac{G}{Ma^3}\right)^{\frac{1}{2}} m_{bh} \quad (22)$$

The authors then derive an equation of motion for a BH given an initial position and velocity similar to Equation 14, with the exception that their definition of β differs slightly from Equation 15 and they do not require the BH to be located at the origin at time zero.

2.3 Large Velocity Kicks

Gualandris & Merritt (2008) also applied the work of Chandrasekhar (1943) to BH dynamics, however instead focussed on the ejections of SMBHs from galaxy cores. Hence the properties of both the BH and the background stellar field considered by Gualandris & Merritt (2008) are different than those addressed in Sections 2.1 and 2.2. The main difference being that Gualandris & Merritt (2008) do not restrict the location of their BH to the inner regions of a stellar field.

Using only the assumption that $m_{bh} \gg m_s$, Gualandris & Merritt (2008) write β as:

$$\beta = 2\pi G^2 \rho(r_{bh}) m_{bh} \ln(1 + \Lambda^2) v_{bh}^{-3} N(< v_{bh}, r) \quad (23)$$

where $\rho(r)$ is the mass density of stars at the BH's position and $N(< v_{bh}, r)$ is the fraction of stars at the BH's position that are moving with velocities less than v_{bh} (in the frame of the galaxy). Since β in Equation 23 is a function of r , the BH's equation of motion cannot be simply set equal to that of the damped oscillator. Hence Gualandris & Merritt (2008) compared the orbital decay of kicked BHs over short time steps in N -body simulations to the decay predicted by $F_{DF} = -\beta v_{bh}$ and Equation 23. The authors found that the work of Chandrasekhar (1943) could initially reproduce the orbital decay of the kicked BH (for $2 < \ln\Lambda < 3$) as long as the evolution of $\rho(r_{bh})$ was accounted for up until when the amplitude of motion falls below the background potential's core radius. Afterwards, Gualandris & Merritt (2008) note that the SMBH and the core oscillate about their center of mass for a long period of time until the oscillations damp to the Brownian level.

Our approach, along with the studies of Gualandris & Merritt (2008) and Chatterjee et al. (2002), determine the equation of motion of the BH by making assumptions regarding the mass of the BH (e.g. $m_{bh} \gg m_{star}$), the kick velocity ($v_k \ll \sigma_{star}$), and its location within the cluster ($r \ll a$) in order to reach an analytic solution. However this significantly limits the BH mass - kick velocity parameter space and leaves many combinations unexplored. Using a suite of N -body models, we will compare each of these approaches to simulations of BHs evolving in star clusters over a range of BH masses and initial kick velocities to identify the regions of parameter space that each study can successfully reproduce and identify the regions of parameter space that need further consideration.

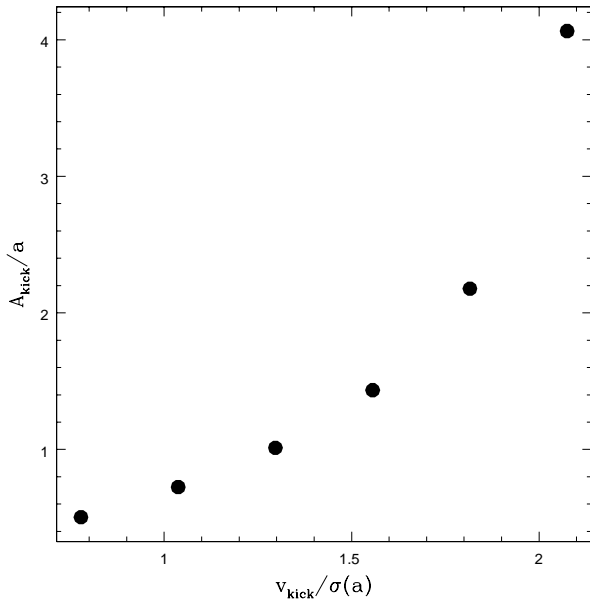


Figure 2. Ratio of initial kick velocity to velocity dispersion at the Plummer scale radius versus the ratio of initial orbital amplitude to the Plummer scale radius for simulations with a range of initial kick velocities (marked in the legend).

3 N-BODY SIMULATIONS

To model the evolution of kicked BHs in star cluster environments, we use the direct N -body code NBODY6 (Aarseth 2003). Each star cluster is initially a Plummer Sphere of 50,000 stars with an initial half-mass radius r_m of 2.5 pc. To isolate and identify the effects of a non-homogeneous stellar field on the orbital evolution of BHs, we assume an equal mass cluster where all stars are $0.5 M_\odot$. Hence model clusters have velocity dispersions and density profiles comparable to open clusters. The kicked BH in each model has a mass of either 10, 50, or $100 M_\odot$ and starts at the center of the cluster with a kick velocity of 3.6, 4.8, 6.0, 7.2, 8.4 or 9.6 km/s. The velocities correspond to $\frac{v_k}{\sigma(a)}$ values of 0.78, 1.0, 1.3, 1.6, 1.8, and 2.0 and are such that the BH does not escape the cluster.

With respect to Figure 1, each of these kicked BHs will behave as under-damped oscillators. Figure 2 illustrates the range in $\frac{v_k}{\sigma(a)}$ and $\frac{A_{kick}}{a}$ covered by our simulations, where A_{kick} is the orbital amplitude associated with v_k calculated explicitly assuming energy is conserved during the time it takes for the BH to travel from the origin to its maximum clustercentric distance.

For illustrative purposes, we have plotted the orbital evolution of the BH in each simulation in Figure 3. In agreement with previous studies, a kicked BH acts as a damped oscillator while its orbit decays due to dynamical friction. The orbits of BHs given low velocity kicks decay much quicker than BHs that are given large velocity kicks, entering the Brownian motion phase at much earlier times. Additionally, consistent with Equation 2, higher mass BHs decay faster than lower mass BHs.

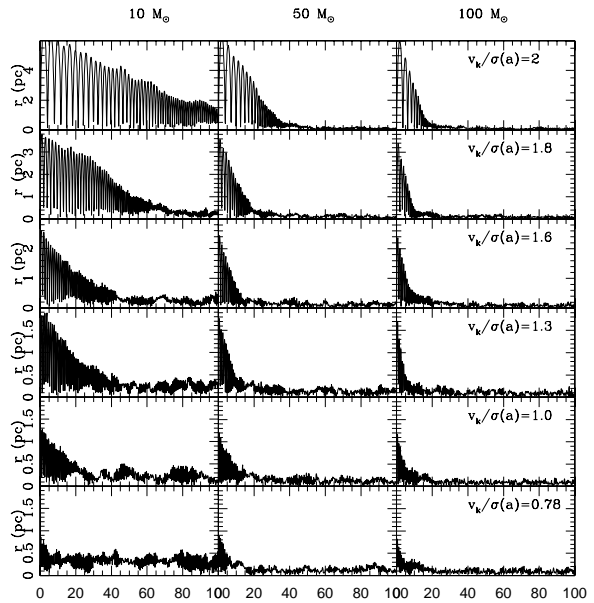


Figure 3. Orbital evolution of kicked BHs with masses of $10 M_\odot$ (left column), $50 M_\odot$ (center column) and $100 M_\odot$ (right column). Different rows correspond to different values of $\frac{v_k}{\sigma(a)}$, which are marked in the legend.

4 COMPARING THEORY TO SIMULATIONS

In order to compare our N -body simulations to the theoretical predictions discussed in Section 2, we first compare the decay of the BH's orbital amplitude in each simulation to the predicted decay rates of Equation 15 (blue) and Equation 22 (red) from Chatterjee et al. (2002). This comparison is made in Figure 4, with the percent difference between the actual and expected decay times noted in each panel. It should be noted that we only plot the BH's decay up to the point that it enters the Brownian motion phase. Once the BH has settled within the core of the cluster and starts undergoing brownian motion, the theoretical predictions are not expected to be representative of the changes in energy experienced by the BHs in our models (Gualandris & Merritt 2008).

From Figure 4, we see that Equations 15 and 22 significantly overestimate how much energy the BH loses via dynamical friction as they yield decay rates much higher than observed in the models. Specifically, both equations predict a much higher energy loss rate when the BH is near its turnaround point in the cluster's core. The discrepancies can be attributed to the fact that both equations assume $v_k \ll \sigma$ and $r \ll a$, which is not the case here, in order to derive an equation of motion for the BH. Even for the lower kick velocity cases, which are closest to the theoretical estimates, only the lowest mass model agrees with dynamical friction theory. The other models are still in disagreement with theoretical estimates because the initial assumption made by Chandrasekhar (1943) that the background stellar field is homogeneous is also not applicable here.

An additional factor that none of the equations account for is energy gains by the BH due to two-body interactions. With the exception of the $\frac{v_k}{\sigma(a)} = 0.78$ models, the

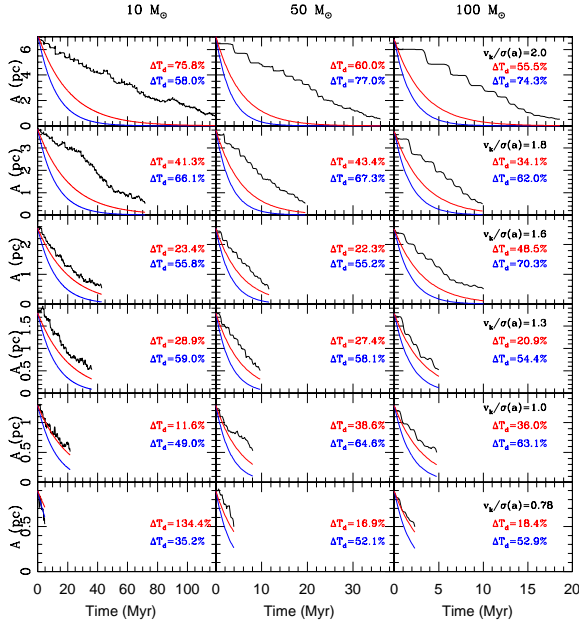


Figure 4. Orbital amplitude of kicked BHs with masses of $10 M_{\odot}$ (left column), $50 M_{\odot}$ (center column) and $100 M_{\odot}$ (right column) as a function of time. Different rows correspond to different values of $\frac{v_k}{\sigma(a)}$, which are marked in the legend. The models are compared to the predictions of Equation 15 (blue) and Equation 22 (red), with the percent difference between the actual and expected decay times noted in each panel.

kicks received by the BHs result in their decay times being longer than the BH’s relaxation time within the cluster. Hence two-body interactions are starting to affect the BHs orbital evolution just as much as, if not more than, dynamical friction. When the BH passes through the dense environment of the cluster’s core, the local potential can vary significantly. When this occurs, major episodes of energy loss and/or gain can occur due to close encounters between the BH and nearby stars. At later times, when the BH’s orbital velocity has decreased it will also be affected by interactions with stars that are travelling faster than the BH itself (Antonini & Merritt 2012; Arca-Sedda & Capuzzo-Dolcetta 2014a; Dosopoulou & Antonini 2017).

Since β in Equation 23 is a function of r , a decay rate cannot be determined using the approach of Gualandris & Merritt (2008). Hence to compare our N -body simulations to Gualandris & Merritt (2008), we instead determine the change in the BH’s energy at each time step and compare it the specific energy loss via the force of dynamical friction acting on the BH. We calculate the specific energy loss predicted by each theory as $\Delta E = -\beta v_{bh} d$, where β is taken from Equation 23 and d is the distance travelled by the BH between time steps. Hence we are assuming F_{DF} is constant between time steps.

From the change in energy predicted by Equation 23 in Figure 5, we see there are significant discrepancies over the course of the BHs decay. In fact, Equation 23 typically underestimates the amount of energy lost by the BH as it passes through the core. This is likely due to the fact that Equation 23 assumes $m_{bh} \gg m_s$ (which

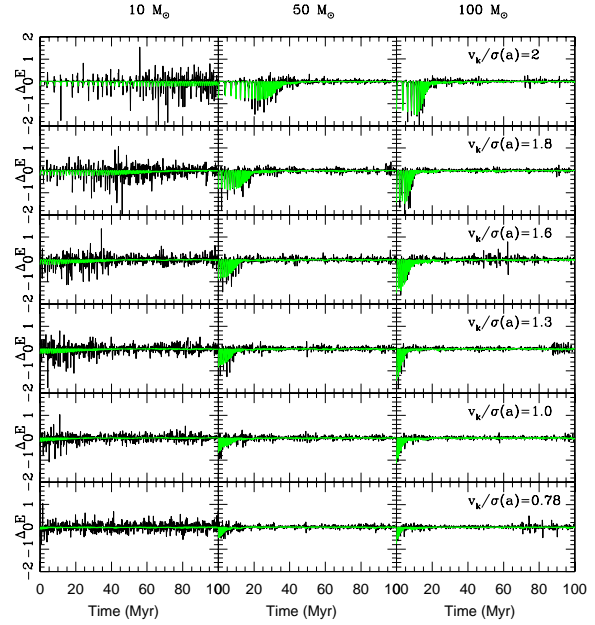


Figure 5. Change in specific energy of kicked BHs with masses of $10 M_{\odot}$ (left column), $50 M_{\odot}$ (middle column) and $100 M_{\odot}$ (right column) as a function of time. Different rows correspond to different values of $\frac{v_k}{\sigma(a)}$, which are marked in the legend. The green line illustrates the predicted change in energy by Gualandris & Merritt (2008).

again is not the case here), since Gualandris & Merritt (2008) does an increasingly better job of matching the simulations as m_{bh} is increased. Furthermore, as previously stated, the fact that the BH sometimes gains energy while passing through the inner regions of the cluster is not taken into account by the works of Chandrasekhar (1943), which Gualandris & Merritt (2008) is based on. With Chandrasekhar (1943) being unable to model changes in the local cluster potential, and the assumptions made by various works leading to both under and over estimating the amount of energy lost by the BH when it passes through denser environments, it appears that the only way to truly dynamically model the effects of dynamical friction on BH evolution over a wide range of BH masses and velocity kicks is knowing the exact form of the stellar distribution function at all times.

5 DISCUSSION

5.1 Two-Body Interactions versus Dynamical Friction

As observed in Figures 4 and 5, classic dynamical friction has trouble predicting the energy change experienced by low-mass BHs passing through the dense core of a stellar population. Equation 15 and Equation 22 both overestimate energy loss due to dynamical friction in the core while the Gualandris & Merritt (2008) model underestimates energy loss. None of the models account for energy gains by the BH due to two-body interactions, which is an important factor in models that have decay times longer

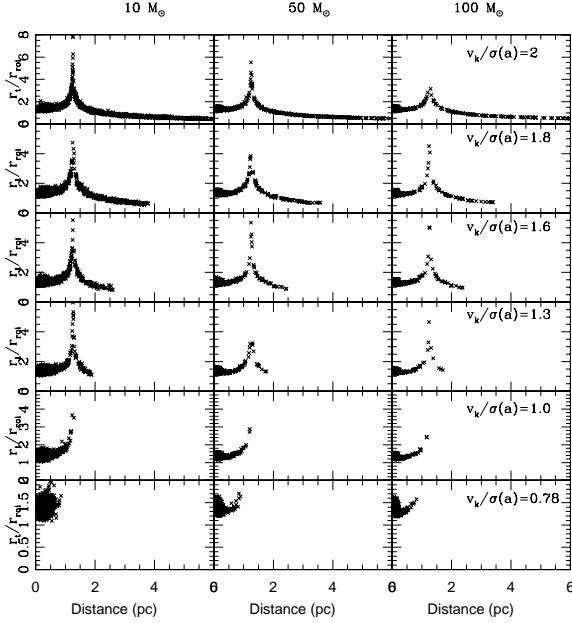


Figure 6. Ratio of BH tidal radius to radius of sphere of influence as a function of clustercentric distance for kicked BHs with masses of $10 M_{\odot}$ (left column), $50 M_{\odot}$ (middle column) and $100 M_{\odot}$ (right column) as a function of time. Different rows correspond to different values of $\frac{v_k}{\sigma(a)}$, which are marked in the legend.

than the BH relaxation time. Two-body interactions are specifically important when the local potential, and fluctuations thereof, experienced by the BH is more dominant than the force due to dynamical friction acting on the BH and when the BH encounters stars with $v > v_{bh}$ (Antonini & Merritt 2012; Arca-Sedda & Capuzzo-Dolcetta 2014a; Dosopoulou & Antonini 2017).

To illustrate where in the star cluster each mechanism dominates, we plot the ratio of the BH’s instantaneous tidal radius r_t to the instantaneous radius of its sphere of influence r_{soi} as a function of clustercentric distance in Figure 6. The BH’s sphere of influence represents a sphere within which the total mass of stars is equal to the mass of the BH. r_t is calculated analytically based on the potentials of both the BH and the cluster ($r_t = (\frac{2.0m_{bh}}{a^2 \Phi(r)/dr^2})^{\frac{1}{3}}$). When r_{soi} is larger than r_t , dynamical friction will be the dominant force acting on the BH as nearby stars are able to respond to the BH’s passing and form a wake behind it. However when r_{soi} is less than r_t , both the motion of the BH and nearby stars are primarily affected by both the strength of and variations in the local potential. Not only will the affects of dynamical friction be minimized, but variations in the local potential can result in the BH gaining or losing energy depending on the direction of its motion and the direction of the net force acting on the BH.

Figure 6 illustrates that in each case $\frac{r_t}{r_{soi}}$ sharply increases near 1.25 pc when the cluster passes in and out of the core, meaning two-body interactions become the dominant source of energy loss/gain for the BH. For the BH masses and kick velocities considered here, when the BH is within 1.25 pc of the cluster’s center it is not surprising that classical dynamical friction will break down. For the lower kick

velocities that Equations 15 and 22 are designed for, since the BHs kinetic energy will be similar to that of background stars the effects of two-body interactions will be minimized. For the case of $m_{bh} \gg 100M_{\odot}$ that Gualandris & Merritt (2008) was designed for, the sphere of influence would be much larger and $\frac{r_t}{r_{soi}}$ would not rise above 1.

5.2 Correcting Orbit Decay

In order to more accurately predict the energy evolution of a kicked BH, we aim to develop either a correction factor or a new formalism that accounts for the assumptions made by classic dynamical friction theory and two-body interactions experienced by the BH within the core of the cluster. Since the true decay rate is less than predicted by Equation 15, we first introduce a correction factor c such that the true decay rate is $\frac{b}{c}$. The parameter c represents a free parameter that we can calculate from simulations in order to compensate for the assumptions of Chandrasekhar (1943) and the additional assumptions we have made in order to derive an analytical description of the BH’s orbital decay (e.g. $v_k \ll \sigma_{star}$ and $r \ll a$). We have elected to correct Equation 15 over Equation 22 due to its treatment of energy lost by the black hole at the turnaround points of its orbit.

To determine the correction factor, we first assume the orbital decay of each BH model in Figure 4 can be treated as an exponential decay of the form

$$A(t) = A_0 e^{-bt/2c} \quad (24)$$

where b is taken from Equation 15. We also consider the case where a BH’s amplitude decays linearly instead of exponentially via:

$$A(t) = \frac{c_L t}{2} + A_0 \quad (25)$$

The orbital decay of each BH simulation and the best fit exponential and linear decay models (found using least squares fitting) are illustrated in Figure 7. The reduced χ^2 values between each fit and the simulated data are noted in each panel.

From Figure 7 it can be seen that for low and intermediate kick velocities ($\frac{v_k}{\sigma} \leq 1.6$), the functional form of the decay is still exponential albeit with a decay rate that is much lower than Equation 15 predicts. The simplified assumption of replacing $\dot{\mathbf{r}}v^{-3}$ with $\dot{\mathbf{r}}(v^2 + \sigma^2)^{-3/2}$ in order to calculate F_{sDF} when $\dot{r} = 0$ is likely a contributing factor to this discrepancy. However, for the majority of cases the linear decay yields a better fit to the simulations (especially for higher mass BHs). In fact, for larger $\frac{v_k}{\sigma}$ ratios the exponential decay approach completely breaks down marking a clear departure from classic dynamical friction theory. Hence only the linear decay formalism is applicable over the entire range of $\frac{v_k}{\sigma}$ presented here.

Using the best fit decay rates to solve for the correction factors c and c_L in each case, we plot the relationship between both factors and $\frac{v_k}{\sigma(a)}$ for all three BH masses in Figure 8. The uncertainty in each fitted decay rate is also plotted in Figure 8.

The lower panel of Figure 8 demonstrates that for

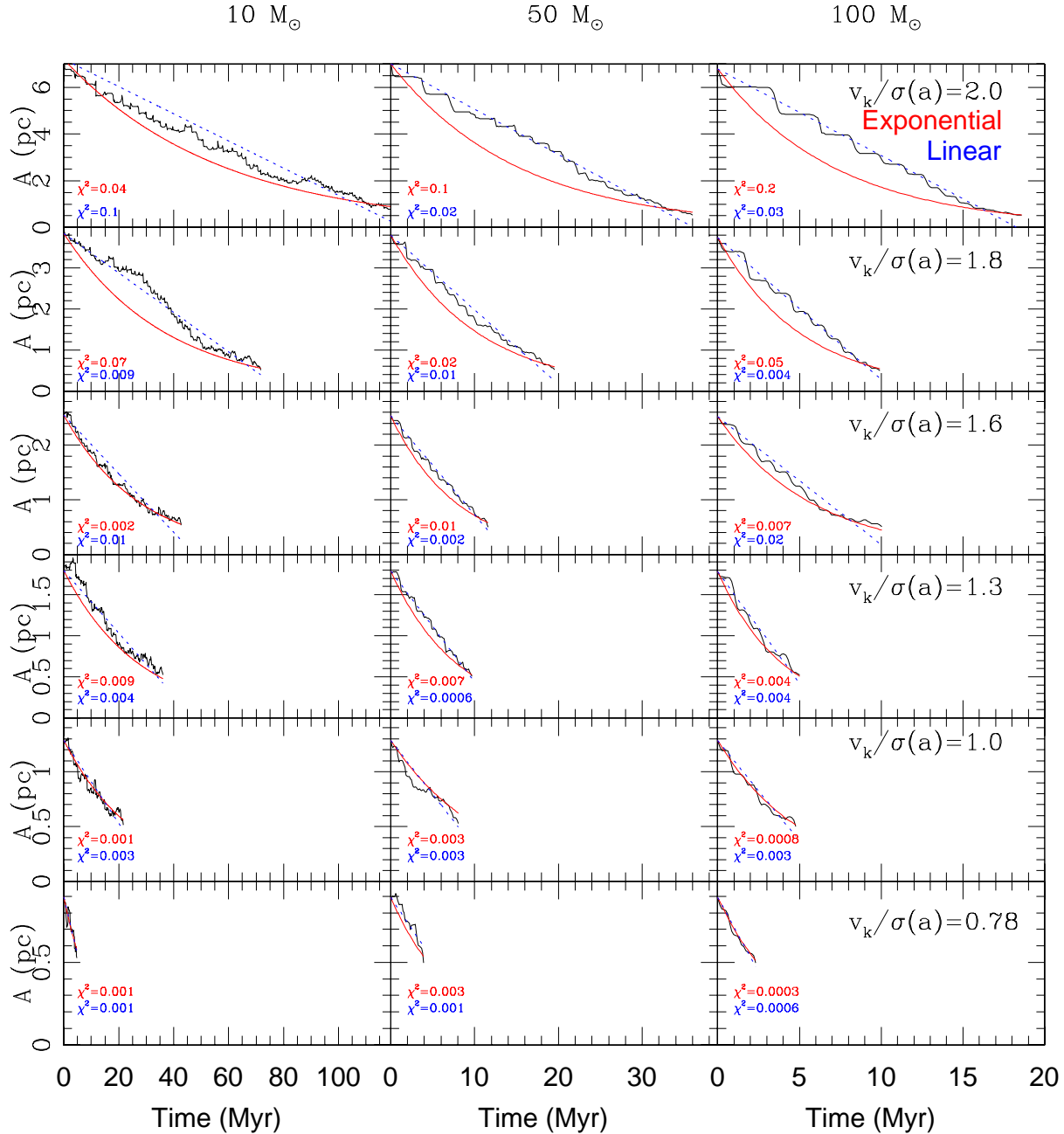


Figure 7. Orbital amplitude of kicked BHs with masses of $10 M_{\odot}$ (left column), $50 M_{\odot}$ (center column) and $100 M_{\odot}$ (right column) as a function of time. Different rows correspond to different values of $\frac{v_k}{\sigma(a)}$, which are marked in the legend. The models are compared to the predictions of Equation 24 (red) and Equation 25 (blue), with the corresponding reduced χ^2 value noted in each panel.

$\frac{v_k}{\sigma} < 1.6$, where the orbital decay is exponential, the decay constant b in Equation 15 needs to be decreased by a factor between one and three. The trend appears to be primarily dependent on kick velocity and independent of BH mass. However there is significant scatter about any function that attempts to relate c to $\frac{v_k}{\sigma}$, likely due to the effects that random close encounters have on the BH's decay rate. For example, a power-law fit to the data has an uncertainty greater than 80%.

It should also be noted that for the case where $m_{bh} =$

$10M_{\odot}$ and $v_k = 3.5$ km/s, the decay is already well fit by an uncorrected decay constant ($c \sim 1$) as both the kick velocity is low and the BH never travels beyond the scale radius of the Plummer sphere. The BH's low mass also means that it is susceptible to two body interactions. Hence it is more accurate to consider the $m_{bh} = 10M_{\odot}$, $\frac{v_k}{\sigma(a)} = 0.78$ model to be in the brownian motion phase at time zero.

The upper panel of Figure 8 illustrates that higher kick velocities ($\frac{v_k}{\sigma} > 1.6$) result in faster mean linear decay rates. For a given BH mass, c_L scales linearly with $\frac{v_k}{\sigma}$ over the

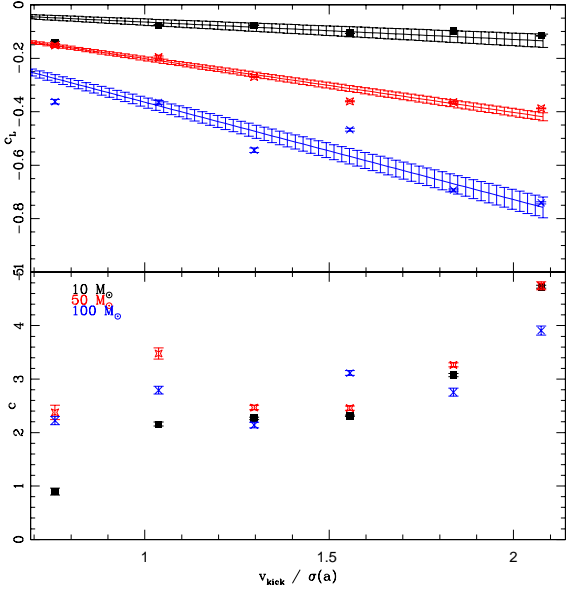


Figure 8. Correction factor c (lower panel) and c_L (upper panel) as a function of $\frac{v_k}{\sigma(a)}$ for BHs with masses of $10 M_\odot$ (black squares), $50 M_\odot$ (red stars) and $100 M_\odot$ (blue crosses). In the upper panel, solid coloured lines represent a linear fit to c_L versus v_k for each BH mass.

entire range covered in the simulations as illustrated by the lines of best fit to each dataset. It is important to note that for each fit we have forced the fits to go through the origin. We also find that the slope of each line of best fit scales linearly with BH mass, such that c_L can be written as:

$$c_L = \left((-0.003 \pm 4.0E-5) * m_{bh} - (0.03 \pm 0.003) \right) \times \frac{v_k}{\sigma} \quad (26)$$

Taking into consideration that the majority of the simulations are better fit by a linear decay rate, and noting that even when an exponential decay is preferred a linear decay still yields a comparable reduced χ^2 , it appears that the orbital decay of kicked BHs with $m_{bh} < 100$ and $\frac{v_k}{\sigma} < 2.0$ is best modelled by Equations 25 and 26. To illustrate the effectiveness of using our correction factor c_L , we plot the corrected theoretical orbital decay of each BH in Figure 9 with the reduced χ^2 value comparing the model to the simulations and the percent difference between the actual and expected decay times noted in each panel.

With the exception of the $m_{bh} = 10 M_\odot - \frac{v_k}{\sigma(a)} = 0.78$ model, Figure 9 illustrates that the linear decay formalism accurately reproduces the orbital decay of a kicked BH. In fact, directly comparing the ΔT_d values in Figure 9 to Figure 4 illustrates that the linear formalism marks a significant improvement over Equations 15 (blue) and Equations 22 (red) for models with $\frac{v_k}{\sigma(a)} > 0.78$. For models with $\frac{v_k}{\sigma(a)} < 0.78$, the assumptions made when deriving Equations 15 and 22 ($v_k < \sigma$, $r < a$) still hold such that either equation can be applied to the lowest kick velocity models. Furthermore, since the decay time is less than the BH relaxation time in the low v_k models, the effects of two-body interactions are minimized. However, some discrepancies between the linear

formalism and the $\frac{v_k}{\sigma(a)} > 0.78$ models remain in select cases when there is a sharp increase or decrease in energy or when the BH starts approaching the Brownian motion phase. In these cases, two-body interactions have become the dominant mechanism behind a BH's orbital evolution. Hence a departure from our dynamical friction model is not surprising.

5.3 Model Limitations

The N -body models presented here have been setup to specifically probe how classical DF theory handles the orbital decay of a kicked BH in a non-homogenous stellar field. The size and mass of our models, selected to optimize computation time, are such that they most directly reflect the evolution of a kicked BH in an open cluster. The applicability of our models to GC and NSCs will depend on multiple factors, mainly the effects of a complete mass spectrum, the total mass and density profile of the cluster, and in the case of NSCs the presence of a central SMBH.

Including a mass spectrum results in the production of an entire BH sub-population and allows for BHs to interact with stars over a range of stellar masses. Interactions with other BHs can cause the in-falling BHs to be kicked from a cluster entirely (Sippel & Hurley 2013), while the presence of a central SMBH has been shown to strongly affect the in-fall process (Antonini & Merritt 2012; Arca-Sedda & Capuzzo-Dolcetta 2014a). Our single-mass model clusters are most comparable to older stellar clusters when the effects of stellar evolution are minimal, other BHs have been kicked from the cluster, and only a strong binary remains (Sippel & Hurley 2013; Spera, Mapelli & Jeffries 2016).

The total mass of our N -body star clusters M_{SC} , the main driver behind the computational time of our models, also limits the ranges of $\frac{m_{bh}}{M_{SC}}$ and $\frac{v_k}{\sigma}$ that we can directly probe as BHs with larger kick velocities will immediately escape the model clusters. Since our models are based on simulations of BHs in stellar fields that are comparable in size and mass to open clusters, additional simulations are required to determine whether the correction factors are scalable to the environments of GCs and NSCs as well. The linear dependence of c_L on m_{bh} and $\frac{v_k}{\sigma}$ suggests scaling to larger values of $\frac{v_k}{\sigma}$ may be possible. However with the linear formalism starting to break down for lower m_{bh} , how our models scale as $\frac{m_{bh}}{M_{SC}}$ decreases requires further study.

6 CONCLUSION

We have used direct N -body simulations of BHs in star clusters to investigate how well classical DF theory predicts the orbital decay of BHs located at the center of a potential well that have received a velocity kick either at formation or due to the anisotropic emission of gravitational waves associated with a BH-BH merger. We specifically focus on BHs with $m_{bh} < 100$, which corresponds to the estimated merger products of the the four gravitational wave detections to date (Abbott et al. 2016,b, 2017,b). Our models indicate that, over the range in BH mass and velocity kick explored here, classical dynamic theory only applies to BHs that receive very small velocity kicks ($\frac{v_k}{\sigma} < 0.78$). In all other

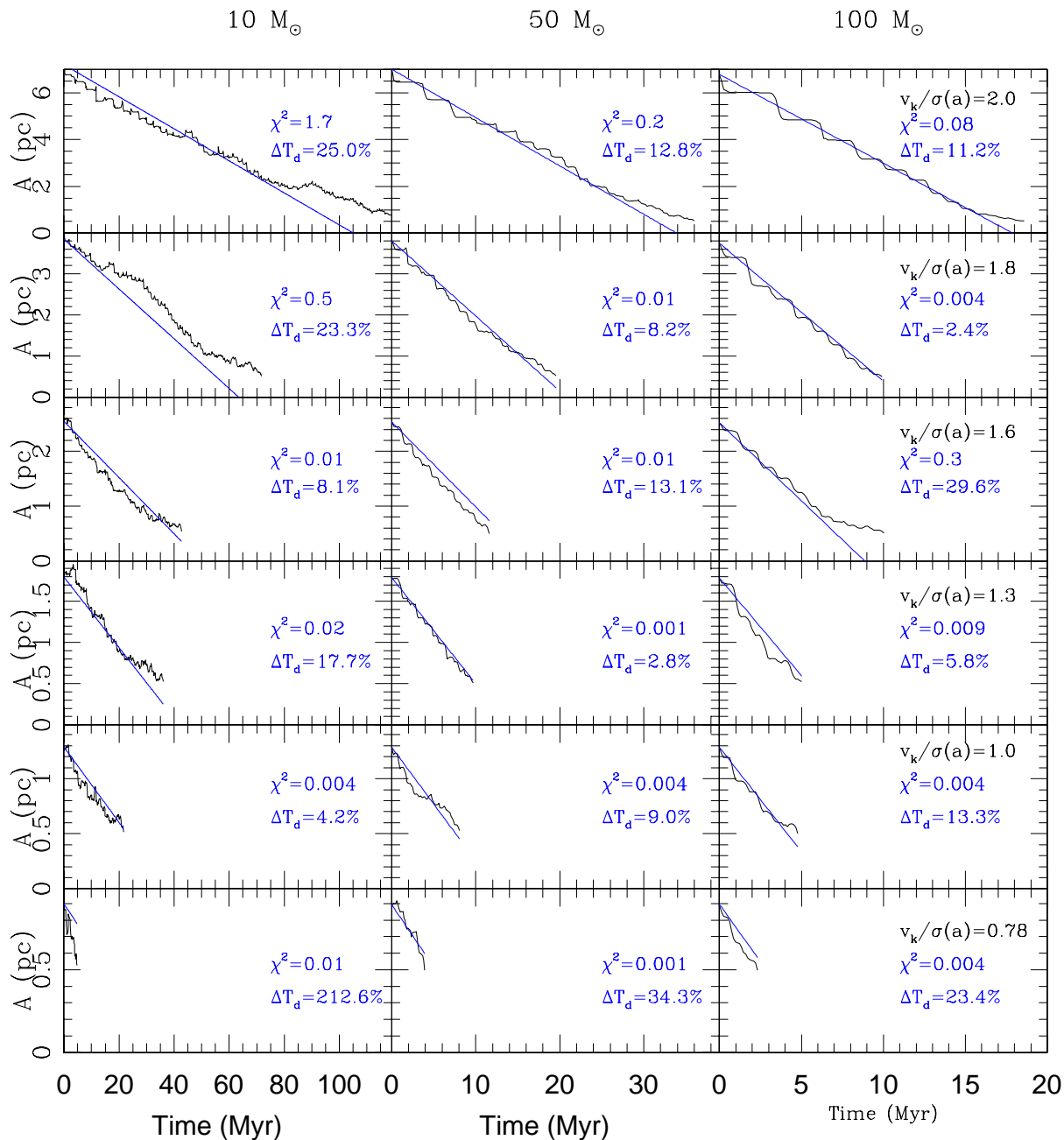


Figure 9. Orbital amplitude of kicked BHs with masses of $10 M_\odot$ (left column), $50 M_\odot$ (center column) and $100 M_\odot$ (right column) as a function of time. Different rows correspond to different values of $\frac{v_k}{\sigma(a)}$, which are marked in the legend. The models are compared to the predictions of Equation 25 with c_L taken from Equation 26 (blue), with the corresponding reduced χ^2 value and percent difference between the actual and expected decay times noted in each panel.

cases, the decay of the BH’s orbit is much slower than predicted.

The discrepancy between classical DF theory and the orbital decay of BHs in our simulations can be attributed to the initial assumptions made by Chandrasekhar (1943) when developing a formalism for dynamical friction and the additional assumptions that need to be made in order to generate an analytical prediction for an orbital decay rate (e.g. Chatterjee et al. 2002; Gualandris & Merritt 2008). More

specifically, DF theory does not account for inhomogeneous background densities, $v_k > \sigma(a)$, $r > a$, and two-body interactions. The latter of which can even result in BHs gaining energy which will further delay orbital decay.

To account for these additional factors, we first attempted to determine a correction factor that can be applied to the exponential decay rate that one would calculate assuming the BH is orbiting within a homogeneous stellar field, $v_k > \sigma(a)$ and $r > a$. However we find that the cor-

rection factor, which is independent of BH mass, can only reproduce the orbital decay of a BH for select cases that have $\frac{v_k}{\sigma} \leq 1.6$. Furthermore, the correction factor has a very weak dependence on $\frac{v_k}{\sigma}$. For all of our $\frac{v_k}{\sigma} \leq 1.6$ models, we find that a linear decay rate can also accurately model a BHs decay and in some cases is even preferred. For $\frac{v_k}{\sigma} > 1.6$, we find that the BH orbits no longer reflect a damped harmonic oscillator and can only be modelled assuming a linear decay rate. Furthermore, the linear decay rate c_L scales linearly with both m_{bh} and $\frac{v_k}{\sigma}$. To directly apply our linear formalism to GCs and NSCs, the influence of stars over an entire mass spectrum, the presence of a central SMBH, and a wider range of cluster masses and density profiles must also be taken into account and requires further study in future work.

Knowing the actual decay time of kicked black holes, which we have shown to be significantly longer than DF theory would predict, directly affects the ability of stellar, intermediate and supermassive BHs to form and grow in dense stellar environments through gravitational wave producing mergers. In fact, the region of the $m_{bh} - \frac{v_k}{\sigma}$ parameter space explored in this study, which is of particular interest for the BHs that have been found to emit gravitational waves upon formation, is in need of a new and dynamically motivated approach for modelling the long term evolution of BHs in star cluster environments. Hence future studies will attempt to isolate the effects of inhomogeneity and the number of two-body interactions on our model.

ACKNOWLEDGMENTS

This work was made possible by the facilities of the Shared Hierarchical Academic Research Computing Network (SHARCNET:www.sharcnet.ca) and Compute/Calcul Canada. N. W. C. L. gratefully acknowledges support from the American Museum of Natural History and the Richard Guilder Graduate School, specifically the Kalbfleisch Fellowship Program, as well as support from a National Science Foundation Award No. AST 11-09395. The authors would also like to kindly thank Mordecai-Mark Mac Low and Enrico Vesperini for useful discussions and suggestions.

REFERENCES

- Aarseth, S.J. 2003, *Gravitational N-body Simulations: Tools and Algorithms* (Cambridge Monographs on Mathematical Physics). Cambridge University Press, Cambridge
- Abbott B. P., et al. 2016, *Phys. Rev. Lett.*, 116, 061102
- Abbott B. P., et al. 2016b, *Phys. Rev. Lett.*, 116, 241103
- Abbott B. P., et al. 2017, *Phys. Rev. Lett.*, 118, 221101
- Abbott B. P., et al. 2017b, *Phys. Rev. Lett.*, 119, 141101, arXiv:1709.09660
- Antonini F., Capuzzo-Dolcetta R., Mastrobuono-Battisti A., Merritt D. 2012, *ApJ*, 750, 111
- Antonini, F. & Merritt, D. 2012, *ApJ*, 745, 83
- Antonini F. 2014, *ApJ*, 794, 106
- Antonini, F. & Rasio, F.A. 2016, *ApJ*, 831, 187
- Arca-Sedda, M. & Capuzzo-Dolcetta, R. 2014a, *ApJ*, 785, 51
- Arca-Sedda, M. & Capuzzo-Dolcetta, R. 2014b, *MNRAS*, 444, 3738
- Arca-Sedda, M., Capuzzo-Dolcetta R., Antonini F., Seth, A. 2015, *ApJ*, 806, 220
- Arca-Sedda, M. 2016, *MNRAS*, 455, 25
- Askar, A., Szkudlarek, M., Gondek-Rosińska, D., Giersz, M., Bulik, T. 2017, *MNRAS*, 464, 36
- Bahcall J. N., Ostriker J. P. 1975, *Nature*, 256, 23
- Banerjee S. 2017, *MNRAS*, 467, 524
- Banerjee S. 2017, *MNRAS*, Accepted, arXiv:1707.00922
- Governato F., Quinn T. R., Wadsley J., Shen S., Volonteri M. 2010, *ApJL*, 721, L148
- Binney J., Tremaine S., 1987, *Galactic Dynamics* (Princeton: Princeton University Press)
- Blecha L., Cox T. J., Loeb A., Hernquist L. 2011, *MNRAS*, 412, 2154
- Blecha L., Sijacki D., Kelley L. Z., Torrey P., Vogelsberger M., Nelson D., Springel V., Snyder G., Hernquist L. 2016, *MNRAS*, 456, 961
- Brockamp, M., Kupper, A.H.W., Thies, I., Baumgardt, H., Kroupa, P. 2014, *MNRAS*, 441, 140
- Bromm V., Loeb A. 2003, *ApJ*, 596, 34
- Chandrasekar S. 1943, *ApJ*, 97, 255
- Chatterjee, P., Hernquist, L., Loeb, A. 2002, *ApJ*, 572, 371
- Chomiuk L., Strader J., Maccarone T. J., Miller-Jones J. C. A., Heinke C., Noyola E., Seth A. C., Ransom S. 2013, *ApJ*, 777, 69
- Cole, D.R., Dehnen, W., Read, J.I., Wilkinson, M.I. 2012, *MNRAS*, 426, 601
- Colpi, M., Mayer, L., Governato, F. 1999, *ApJ*, 525, 720
- Comerford J. M., Schluns K., Greene J. E., Cool R. J. 2013, *ApJ*, 777, 64
- Deane R. P., Paragi Z., Jarvis M. J., Coriat M., Bernardi G., Fender R. P., Frey S., Heywood I., Klöckner H.-R., Grainge K., Rumsey C. 2014, *Nature*, 511, 57
- Dosopoulou F., Antonini F. 2017, *ApJ*, 840, 31
- Doyon R., Hutchings J. B., Beaulieu M., Albert L., Lafrenière D., Willott C., Touahri D., Rowlands N., Maszkiewicz M., et al. 2012, *SPIE*, 8442, 2R
- Favata M., Hughes S. A., Holz D. E. 2004, *ApJ*, 607, L5
- Ford K. E. S., McKernan B., Sivaramakrishnan A., Martel A. R., Koekemoer A., Lafrenière D., Parmentier S. 2014, *ApJ*, 783, 73
- Fujii, M., Funato, Y., Makino, J. 2006, *PASJ*, 58, 743
- Graham M. J., Djorgovski S. G., Stern D., Drake A. J., Mahabal A. A., Donalek C., Glikman E., Larson S., Christensen E. 2015, *MNRAS*, 453, 1562
- Gratton R. G., Carretta E., Bragaglia A. 2012, *A&ARv*, 20, 50
- Gualandris A., Merritt D. 2008, *ApJ*, 678, 780
- Guedes J., Madau P., Mayer L., Callegari S. 2011, *ApJ*, 729, 125
- Haiman Z., Loeb A. 2001, *ApJ*, 552, 459
- Islam R. R., Taylor J. E., Silk J. 2003, *MNRAS*, 340, 647
- Just A., Khan F. M., Berczik P., Ernst A., Spurzem R. 2011, *MNRAS*, 411, 653
- Kroupa, P., Tout C.A., Gilmore, G. 1993, *MNRAS*, 262, 545
- Kroupa P. 2001, *MNRAS*, 322, 231
- Lauer T. R., et al. 1998, *AJ*, 116, 2263
- Leigh N. W. C., Sills A., Knigge C. 2007, *ApJ*, 661, 210
- Leigh N. W. C., Sills A., Knigge C. 2009, *MNRAS*, 399,

- L179
- Leigh N. W. C., Sills A. 2011, MNRAS, 415, 1410
- Leigh N., Sills A., Knigge C. 2011, MNRAS, 410, 2370
- Leigh N. W. C., Geller A. M. 2012, MNRAS, 425, 2369
- Leigh N. W., Mastrobuono-Battisti A., Perets H. B., Böker T. 2013, MNRAS, 441, 919 (Leigh et al. 2013a)
- Leigh N. W. C., Böker T., Maccarone T. J., Perets H. B. 2013, MNRAS, 429, 2997 (Leigh et al. 2013b)
- Leigh N. W. C., Giersz M., Webb J. J., Hypki A., De Marchi G., Kroupa P., Sills A. 2013, MNRAS, 436, 3399 (Leigh et al. 2013c)
- Leigh N. W. C., Lützgendorf N., Geller A. M., Maccarone T. J., Heinke C., Sesana A. 2014, MNRAS, 444, 29
- Leigh N. W. C., Giersz M., Marks M., Webb J. J., Hypki A., Heinke C. O., Kroupa P., Sills A. 2015, MNRAS, 446, 226
- Leigh N. W. C., Geller A. M., Toonon S. 2016, ApJ, 818, 21
- Mac Low M.-M., McCray R., Norman M. L. 1989, ApJ, 337, 141
- Mac Low M.-M., van Buren D., Wood D. O. S., Churchwell E. 1991, ApJ, 369, 395
- Maccarone T. J., Kundu A., Zepf S. E., Rhode K. L. 2007, Nature, 445, 183
- Madau P., Rees M. J. 2001, ApJL, 784, L38
- Madau P., Rees M. J., Volonteri M., Haardt F., Oh S. P. 2004, ApJ, 604, 484
- Maeder A. 2009, Physics, Formation and Evolution of Rotating Stars. Berlin: Springer-Verlag
- McKernan B., Ford K. E. S., Kocsis B., Haiman Z. 2013, MNRAS, 432, 1468
- McKernan B., Ford K. E. S. 2015, MNRAS, 452, 1
- McKernan B., et al., 2017, submitted (arXiv:1702.07818)
- Merritt D., Milosavljevic M., Favata M., Hughes S. A., Holz D. E. 2004, ApJL, 607, L9
- Merritt D. 2013, Dynamics and Evolution of Galactic Nuclei (Princeton: Princeton University Press)
- Miller, M. C., Lauburg, V. M. 2008, ApJ, 692, 917
- Oh S. P., Haiman Z. 2002, ApJ, 569, 558
- Ostriker, J.P., Binney J., Saha, P. 1989, MNRAS, 241, 849
- Ostriker E. 1999, ApJ, 513, 252
- Penarrubia J., Just A., Kroupa P. 2004, MNRAS, 349, 747
- Pesce, E., Capuzzo-Dolcetta R., Vietri, M. 1992, MNRAS, 256, 368
- Peuten, M., Zocchi, A., Gieles, M., Gualandris, A., Hénault-Brunet, V. 2016, MNRAS, 462, 2333
- Pfahl, E., Rappaport, S., Podsiadlowski, P. 2002, ApJ, 573, 283
- Pfahl, E. 2003 in KITP Conference: Globular Clusters, Formation, Evolution and the Role of Compact Objects, January 29, 2003, Kavli Institute for Theoretical Physics, University of California, Santa Barbara
- Portegies Zwart S. F., Baumgardt H., Hut P., Makino J., McMillan S. L. W. 2004, Nature, 428, 724
- Read J. I., Geordt T., Moore B., Pontzen A. P., Stadel J. 2006, MNRAS, 373, 1451
- Repetto S., Davies, M.B., Sigurdsson, S. 2012, MNRAS, 425, 2799
- Rodriguez, C. L., Morscher, M., Pattabiraman, B., Chatterjee, S., Haster, C.-J., and Rasio, F. A. 2015, Physical Review Letters, 115, 051101
- Rodriguez, C. L., Chatterjee, S. and Rasio, F. A. 2016, Physical Review Letters, 93, 084029
- Salpeter, E.E. 1955, ApJ, 121, 161
- Shang C., Bryan G. L., Haiman Z. 2010, MNRAS, 402, 1249
- Shapiro S. L. 2005, ApJ, 620, 59
- Shih I. C., Kundu A., Maccarone T. J., Zepf S. E., Joseph T. D. 2010, ApJ, 721, 323
- Sippel, A.C. & Hurley, J.R. 2013, MNRAS, 430, L30
- Sivaramakrishnan A., Lafrenière D., Ford K. E. S., McKernan B., Cheetham A., Greenbaum A. Z., Tuthill P. G., Lloyd J. P., Ireland M. J., et al. 2012, SPIE, 8442, 2S
- Spera M., Mapelli M., Jeffries R.D. 2016, MNRAS, 460, 317
- St. Laurent K. E., Greenbaum A. Z., Ygouf M., Sivaramakrishnan A., Mugnier L., McKernan B., Ford, K. E. S.; to be submitted to ApJ 2016
- Strader J., Chomiuk L., Maccarone T. J., Miller-Jones J. C. A., Seth A. C. 2012, Nature, 490, 71
- Tanaka T. L., Haiman Z. 2009, ApJ, 696, 1798
- Tanaka T. L., Li M. 2014, MNRAS, 439, 1092
- Tayler R. J., Wood P. R. 1975, MNRAS, 171, 467
- Tremaine S. D., Ostriker J. P., Spitzer L. Jr. 1975, ApJ, 196, 407
- Trenti M., van der Marel, R. 2013, MNRAS, 435, 3272
- Vicari A., Capuzzo-Dolcetta R., Merritt, D. 2007, ApJ, 662, 797
- Volonteri M., Haardt F., Madau P. 2003, ApJ, 582, 559
- Volonteri M., Rees M. J. 2005, ApJ, 633, 624
- Volonteri M., Rees M. J. 2005, ApJ, 650, 669
- Wise J. H., Abel T. 2007, ApJ, 685, 40
- Wrobel J. M., Walker R. C., Fu H. 2014, ApJ, 792, 8

This paper has been typeset from a \TeX / \LaTeX file prepared by the author.